Chemical Science

ROYAL SOCIETY OF CHEMISTRY

EDGE ARTICLE

View Article Online
View Journal | View Issue



Cite this: *Chem. Sci.*, 2021, **12**, 9946

All publication charges for this article have been paid for by the Royal Society of Chemistry



# Cyclic monoterpenes trapped in a polyaromatic capsule: unusual selectivity, isomerization, and volatility suppression†

Ryuki Sumida,[a] Yuya Tanaka,[a] Keita Niki,[a] Yoshihisa Sei,[a] Shinji Toyota[b] and Michito Yoshizawa*[a]

Received 9th April 2021
Accepted 17th May 2021

DOI: 10.1039/d1sc01987b

rsc.li/chemical-science

Cyclic monoterpenes (CMTs) are intractable natural products with high volatility and strong odors so that there has been no molecular receptor capable of selectively and tightly trapping CMTs in both solution and the solid state. We herein report that a polyaromatic capsule acts as a functional nanoflask for CMTs with the following five features: (i) the capsule can selectively bind menthone from mixtures with other saturated CMTs in water. In contrast, (ii) treatment of the capsule with mixtures of menthone and π-conjugated CMTs gives rise to ternary host–guest complexes with high pair-selectivity. Notably, (iii) the encapsulated menthone displays unusual isomerization from a typical chair conformer to otherwise unstable conformers upon heating. (iv) The selective binding of volatilized CMTs is demonstrated by the capsule even in the solid state at atmospheric pressure. Furthermore, (v) the volatilities of CMTs are significantly suppressed at elevated temperatures by the capsule upon encapsulation in solution as well as in the solid state.

## Introduction

Cyclic monoterpenes (CMTs) are simple yet important natural products, selectively biosynthesized from an acyclic monoterpene derivative in plants (Fig. 1a).[1] The bioproducts are widely used as common fragrances, essences, and perfumes, due to their characteristic odors, and as key starting materials for drug synthesis.[2,3] The relatively small structures (*i.e.*, ~0.7 nm and ~200 Da) and the absence of strongly interactive substituents make CMTs highly volatile. Thus, these intractable features cause great difficulty in their molecular-level recognition and microscale separation from CMT mixtures, besides the existence of plenty of derivatives with only tiny structural differences.[4] There have been many reports on molecular receptors (*e.g.*, covalent tubular and bowl-shaped compounds,[5] hydrogen-bonding and coordination capsules,[6] and π-stacking capsules[7]) capable of binding CMTs such as camphor (**CMP**), menthol (**MTL**), and *p*-cymene (**CMN**; Fig. 1a). However, the majority of the previous receptors possess open and/or flexible cavities surrounded by aliphatic and/or small aromatic

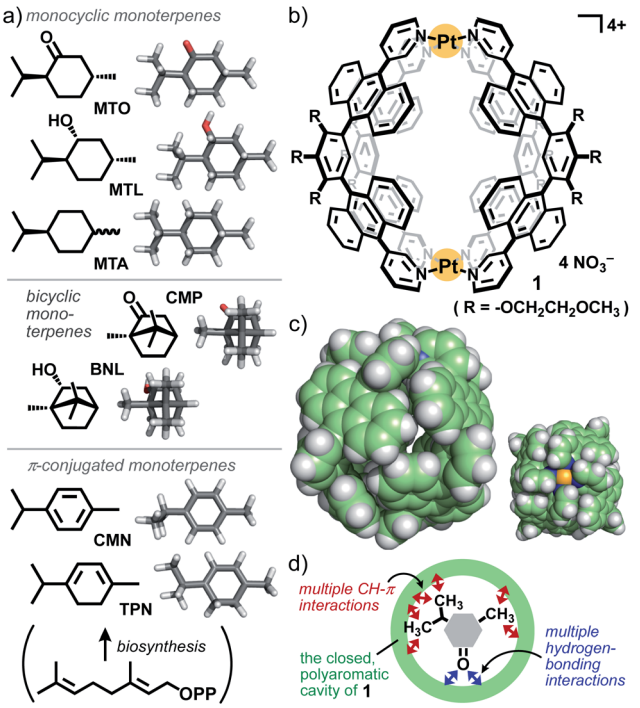


Fig. 1 (a) Cyclic monoterpenes (CMTs; OPP = pyrophosphate) and (b) polyaromatic capsule **1** used in this work as volatile biosubstrates and a receptor, respectively. (c) Crystal structure of **1** (top and side views; the hydrophilic side chains are replaced by hydrogen atoms for clarity). (d) Strategy for the selective recognition of CMTs by **1**.

[a]*Laboratory for Chemistry and Life Science, Institute of Innovative Research, Tokyo Institute of Technology, 4259 Nagatsuta, Midori-ku, Yokohama 226-8503, Japan. E-mail: yoshizawa.m.ac@m.titech.ac.jp*

[b]*Department of Chemistry, School of Science, Tokyo Institute of Technology, 2-12-1 Ookayama, Meguro-ku, Tokyo 152-8551, Japan*

† Electronic supplementary information (ESI) available. CCDC 2058897 and 2059097. For ESI and crystallographic data in CIF or other electronic format see DOI: 10.1039/d1sc01987b

frameworks[5–8] so that the selective recognition and high volatility suppression of CMTs have been hardly accomplished by the artificial receptors so far. What type of molecular receptor is the most suitable for these bioproducts? We herein focused on polyaromatic capsule **1** (Fig. 1b and c) to strategically utilize multiple CH–π and hydrogen-bonding interactions with CMTs in the closed cavity (Fig. 1d).

Capsule **1**, with a simple $M_2L_4$ composition, provides a spherical cavity with relatively high rigidity and a diameter of ~1 nm (Fig. 1b),[9] in contrast to biological cavities with high flexibility and complex shapes. In water, the polyaromatic cavity of **1** binds various biomolecules, *e.g.*, relatively large androgens (~1.4 nm in length) and medium-sized xanthines and disaccharides (~1.0 nm in length), with a high selectivity through efficient host–guest interactions.[10] Here we disclose that, unlike the previous receptors,[5–8] capsule **1** acts as a functional nanoflask toward relatively small CMTs with the following novel characteristics. (i) The capsule binds menthone (**MTO**; Fig. 1a) with high efficiency and selectivity from mixtures with other saturated CMTs (*e.g.*, **MTL** and **CMP**) in water at room temperature. The host–guest structure is fully confirmed by NMR, MS, ITC, and X-ray crystallographic analyses. On the other hand, (ii) **MTO** is pair-selectively bound by **1** with π-conjugated CMTs (*i.e.*, **CMN** and **TPN**) under the same conditions. In the confined cavity, (iii) unusual thermal isomerization of **MTO** from a typical diequatorial chair conformer to otherwise unstable diaxial chair and twist-boat conformers can be observed in a quantitative and reversible fashion. The cavity-directed, conformational stabilization of the resultant isomers is supported by theoretical calculations. (iv) The selective binding of volatilized **MTO** is also accomplished by solid **1** at ambient temperature and pressure. Finally, we reveal that (v) capsule **1** significantly suppresses the volatilities of CMTs upon encapsulation in solution as well as in the solid state. Combined with the crystal structures, the present behaviour demonstrates the presence of highly efficient CH–π and hydrogen-bonding interactions between the polyaromatic host cavity and the CMT guests.

## Results and discussion

### Selective trap of CMTs by the capsule in water

Capsule **1** bound various CMTs to give the corresponding 1 : 1 host–guest complexes in a quantitative fashion and displayed a distinct binding preference. When a mixture of (−)-menthone (**MTO**), *p*-menthane (**MTA**), and (−)-menthol (**MTL**; 10 equiv. each) was suspended in a $D_2O$ solution (0.5 mL) of **1** (0.26 μmol) at room temperature for 1 h, host–guest complexes **1**·**MTO**, **1**·**MTA**, and **1**·**MTL** were formed in 90, 10, and 0% yields, respectively (Fig. 2a, left).[11] In the $^1$H NMR spectrum, the three methyl and six methylene signals of encapsulated **MTO** were observed in the range of −2.65 to −0.71 ppm. These guest signals are outstandingly shifted upfield, due to the efficient shielding effect ($\Delta\delta_{max} = -4.09$ ppm) of the polyaromatic host (Fig. 2b and c). Selective formation of **1**·**MTO** was further confirmed by the ESI-TOF MS spectrum, showing a series of prominent peaks derived from the $[\mathbf{1}\cdot\mathbf{MTO}–n\cdot NO_3^-]^{n+}$ species

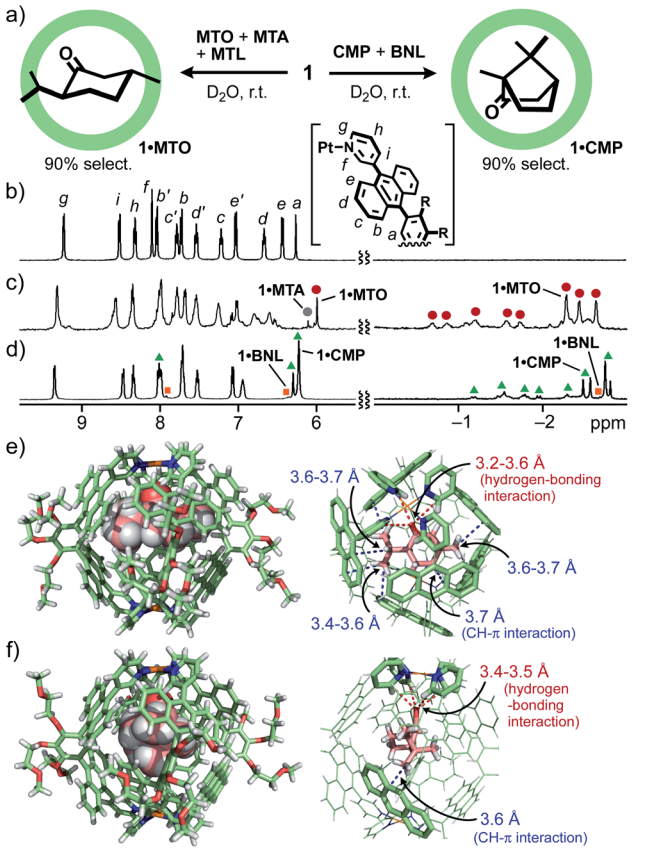


Fig. 2 (a) Selective binding of MTO from a mixture of MTO, MTA, and MTL (left side) and CMP from a mixture of CMP and BNL (right side) by 1. $^1$H NMR spectra (500 MHz, $D_2O$, r.t.) of (b) 1 and host–guest complexes obtained from mixtures of (c) 1, MTO, MTA, and MTL, and (d) 1, CMP, and BNL after 1 h at r.t. X-ray crystal structures of (e) 1·MTO and (f) 1·CMP, and their host–guest interactions.

($n$ = 4 to 2; Fig. S4†). A similar binding study clarified that **1** binds **MTA** stronger than **MTL** (in a 67 : 33 ratio; Fig. S17†).[11] Therefore, the present competitive experiments elucidated the binding preference in the order of **MTO** ≫ **MTA** > **MTL**. The binding constant ($K_a$) of **1** toward **MTO** was estimated to be $6.6 \times 10^5$ $M^{-1}$ by isothermal titration calorimetry (ITC) analysis (Fig. S20 and Table S1†).[11] The obtained thermodynamics indicate that the guest binding is an enthalpically favorable process ($\Delta H = -84.5$ kJ mol$^{-1}$, $T\Delta S = -51.5$ kJ mol$^{-1}$ (25 °C)), through multiple host–guest interactions.

Whereas bicyclic monoterpenes such as (−)-camphor (**CMP**) and (−)-borneol (**BNL**) were also quantitatively bound by **1** in water (Fig. S9–S13†), their binding affinities were lower than those of the monocyclic ones. Treatment of a mixture of **CMP** and **BNL** (10 equiv. each) with **1** in $D_2O$ gave rise to **1**·**CMP** and **1**·**BNL** in a 9 : 1 ratio (Fig. 2a, right and 2d).[12] Since **1** bound **MTL** more efficiently (65% selectivity) than **CMP** from a 1 : 1 **MTL**/**CMP** mixture (Fig. S19†),[11] the present competitive studies established the binding affinities of **1** for the tested CMTs to be **MTO** ≫ **MTA** > **MTL** > **CMP** ≫ **BNL**. This order stems not from the guest solubility in water (Fig. S23†) but from the identity of the guest shape and substituents. High recognition ability of **1**

toward **MTO** most probably results from its planar structure (0.9 nm in the longest length) with three methyl groups and one carbonyl group (Fig. 1d). Eventually, the X-ray crystallographic analysis of **1**·**MTO** indicated that the functional groups of **MTO**, adopting a typical diequatorial chair conformer, efficiently interact with the polyaromatic host cavity through seven CH–π and four CH···O=C hydrogen-bonding interactions (Fig. 2e).[10c,13] The number of the observed host–guest interactions within **1**·**MTO** is larger than that within **1**·**CMP** (*i.e.*, one CH–π and four CH···O=C interactions; Fig. 2f), which is consistent with the ITC data in solution ($\Delta H$ = −84.5 and −14.9 kJ mol$^{-1}$, respectively).[11,12] The spherical structure of **CMP** (~0.6 nm in diameter) is too small to efficiently contact with the spherical cavity (~1.0 nm) of **1**.

### Pairwise encapsulation of CMTs by the capsule

Pairwise encapsulation of CMTs exceptionally took place, when **1** was combined with **MTO** and π-conjugated CMTs, such as *p*-cymene (**CMN**) and α-terpinene (**TPN**), in water.[14] Although there is no electrostatic interaction between **MTO** and **CMN**, ternary host–guest complex **1**·(**MTO**·**CMN**) was generated exclusively from a 1 : 1 mixture of **MTO** and **CMN** (10 equiv. each), being stirred in a $D_2O$ solution of **1** (0.52 mM) at room temperature for 1 h (Fig. 3a, left). The $^1$H NMR spectrum of the product displayed new signals derived from the host and the two guests (Fig. 3c), which are completely different from those of **1**·**MTO** and **1**·(**CMN**)$_2$, prepared separately (Fig. 3b and d, respectively). The formation of the ternary complex was indicated by ESI-TOF MS analysis, where the MS peaks corresponding to [**1**·(**MTO**·**CMN**)–*n*·$NO_3^-$]$^{n+}$ (*n* = 4 to 2) species were observed at *m*/*z* = 976.6, 1322.4, and 2014.6 (Fig. 3e).[14] The 1 : 1 ratio of guests **MTO** and **CMN** within **1** was further confirmed by $^1$H NMR analysis after extraction of the encapsulated guests with $CDCl_3$. Notably, the selective formation of **1**·(**MTO**·**CMN**) (>98%) was found even using a 1 : 5 : 50 mixture of **1**, **MTO**, and **CMN** in water at room temperature (Fig. S28†).[11]

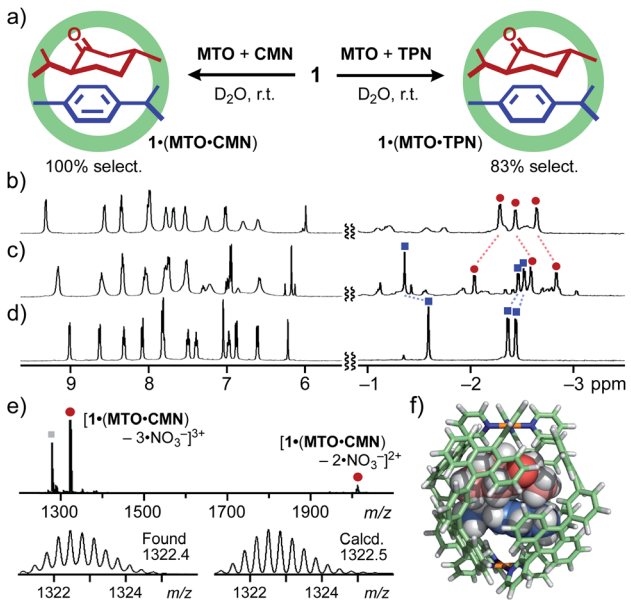


Fig. 3 (a) Selective formation of ternary host–guest complexes **1**·(**MTO**·**CMN**) and **1**·(**MTO**·**TPN**). $^1$H NMR spectra (500 MHz, $D_2O$, r.t.) of (b) **1**·**MTO**, (c) **1**·(**MTO**·**CMN**), and (d) **1**·(**CMN**)$_2$. (e) ESI-TOF MS spectrum ($H_2O$) of **1**·(**MTO**·**CMN**) (gray square: **1**·**MTO**) and the expanded and simulated signals of [**1**·(**MTO**·**CMN**)–3$NO_3^-$]$^{3+}$. (f) Optimized structure of **1**·(**MTO**·**CMN**) (R = −H).

The observed pair-selectivity is ascribed to structure-based complementary guest uptake. The optimized structure of **1**·(**MTO**·**CMN**) suggested that the size and shape of a stacked heterodimer of planar **MTO** (diequatorial chair form) and **CMN** nicely fit those of the polyaromatic cavity of **1** (Fig. 3f).[15] The π-conjugated framework of **CMN** is essential for the pair-selective encapsulation with **MTO** so that **1**·(**MTO**·**TPN**) also formed in high selectivity (83%) by the treatment of **1** with **MTO** and **TPN**, bearing a cyclohexadiene ring, under the same conditions (Fig. 3a, right). In contrast, the formation of a ternary complex was undetected from a mixture of **1**, **MTO**, and **MTA** under various conditions (Fig. S15†).

### Thermal isomerization of menthone within the capsule

In the confined cavity of **1**, a unique conformation change of **MTO** was observed from a typical chair form to otherwise labile forms by thermal stimuli. In the $^1$H NMR spectra of **1**·**MTO** in $D_2O$, unexpectedly, the aromatic host signals and the aliphatic guest signals were fully shifted upon heating at 100 °C for 8 h, without the appearance of empty host signals (Fig. 4a and b, left). Particularly, the downfield shift of the inner protons ($H_a$) of **1** and its splitting into three signals suggested the generation of three new species derived from **MTO** in the cavity.[16] The IR analysis of **1**·**MTO** showed the C=O stretching band of the encapsulated **MTO** being also shifted by 10 cm$^{-1}$ through the heating (Fig. S36†). On the other hand, the ESI-TOF MS peaks of the host–guest complex were unchanged before and after the treatment (Fig. 4a and b, right). The new host and guest NMR signals gradually went back to the initial positions at 30 °C ($\tau_{1/2}$ = 22 h; Fig. S37d†).[11,17] The signal shifts could be repeated at least three times without the decomposition of the host–guest complex (Fig. S37c†). These findings indicate the thermal isomerization of **MTO** in the cavity of **1** in water.

Theoretical calculation studies suggested the formation of diaxial-type chair isomer **ACI** and twist-boat isomers **TBI-a** (major) and **TBI-b** (minor) upon heating and their large conformational stabilization within **1** (Fig. 4c).[11,18] Whereas the energy of **ACI** is 13.6 kJ mol$^{-1}$ higher than that of **MTO** (diequatorial-type chair form) without **1** (Fig. 4c), the energy difference ($\Delta E$) between **1**·**ACI** and **1**·**MTO** decreased to be 5.7 kJ mol$^{-1}$ (Fig. 4d). Accordingly, the diaxial chair conformer was stabilized by 7.9 kJ mol$^{-1}$ upon encapsulation, as compared with the diequatorial chair conformer. Conformers **TBI-a** and **TBI-b** are also stabilized by 10.0 and 6.0 kJ mol$^{-1}$ within **1**, respectively. In the optimized structures, roughly bowl-shaped **ACI** and **TBI** are suitably accommodated in the spherical cavity of **1** (Fig. 4d), displaying multiple host–guest CH–π and hydrogen-bonding interactions (Fig. S40b†). To the best of our knowledge, there has been no report on the spectroscopic observation of the diaxial to diequatorial[19] and chair to twist-

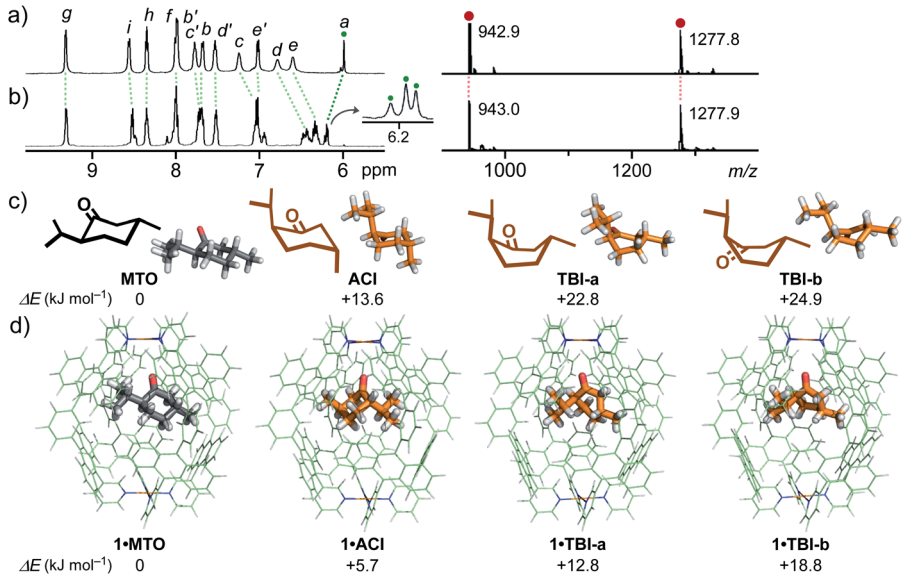


Fig. 4 $^1$H NMR spectra (500 MHz, $D_2O$, r.t., left) and ESI-TOF MS spectra ($H_2O$, right) of **1**·**MTO** (a) before and (b) after heating at 100 °C for 8 h. (c) Optimized structures of **MTO**, **ACI**, **TBI-a**, and **TBI-b** (c) without **1** and (d) within **1**, and their relative energies based on **MTO** or **1**·**MTO** (the peripheral substituents are replaced with hydrogen atoms for clarity).

boat isomerizations[20] of CMTs as well as other cyclohexane derivatives in solution.

### Selective trap of volatilized CMTs by the capsule solid

Inspired by the solution-state binding ability of **1** toward CMTs, we next examined the binding of volatilized CMTs using solid **1**.[21,22] To our surprise, a solid of **1** could efficiently and selectively bind **MTO** from a mixture with volatilized CMTs at room temperature and atmospheric pressure. Each of **MTO**, **MTA**, and **MTL** (100 equiv.) was placed in a closed glass vessel (50 mL) including **1** (0.26 μmol) without direct host–guest contact (Fig. 5a). After standing for 14 h, the resultant solid was exposed to reduced pressure (480 Pa, 1 h) to remove CMTs outside the solid. The guest binding and its selectivity were elucidated by $^1$H NMR analysis in $D_2O$. The NMR spectrum indicated that **1** binds the guests quantitatively to yield host–guest complexes **1**·**MTO**, **1**·**MTL**, and **1**·**MTA** in 70, 30, and 0%, respectively (Fig. 5b). Solid **1** also bound volatilized **MTO** and **CMN** pair-selectively to give **1**·(**MTO**·**CMN**) in 95% yield after standing for 2 d (Fig. 5c).

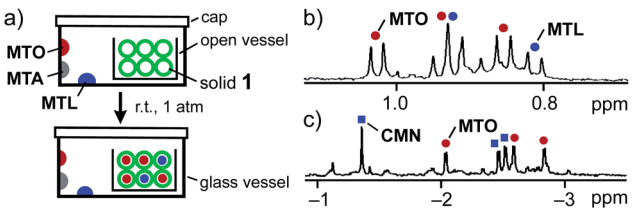


Fig. 5 (a) Selective binding of volatilized **MTO** from a mixture of CMTs by solid **1**. (b) $^1$H NMR spectrum (400 MHz, $CDCl_3$, r.t.) of guests extracted from solid **1** after treatment with **MTO**, **MTA**, and **MTL**. (c) $^1$H NMR spectrum (500 MHz, $D_2O$, r.t.) of host–guest complexes obtained from a mixture of solid **1** and volatilized **MTO** and **CMN**.

It is noteworthy that each of the tested CMTs was quantitatively encapsulated by **1** in water, as described above, whereas solid **1** displayed largely different affinity toward each of the volatilized CMTs, *e.g.*, quantitative binding to **MTO** yet weak binding to **CMP** (4%) under the same conditions (Fig. S45†). The rigid and sterically demanding features of **CMP** are major reasons for the selectivity.

### Volatility suppression of CMTs by the capsule

Notably, the volatility of CMTs was largely suppressed upon encapsulation by **1** in both solution and the solid state. When a mixture of **1**·**CMP** and **CMP** (~12 equiv.) in $D_2O$ was heated at 80 °C, the majority of free **CMP** (96%) was volatilized after 25 h. On the other hand, **CMP** within **1** remained fully intact under the same conditions, as confirmed by time-dependent $^1$H NMR and ESI-TOF MS analyses (Fig. 6a and b).[11] No peaks derived from empty **1** were detected in the MS spectrum. On the basis of the NMR studies, the kinetic analysis of the guest volatilization revealed that the half-lives ($\tau_{1/2}$) of free and encapsulated **CMP** are approximately 5 and >690 h, respectively (Fig. 6c), indicating an encapsulation-induced >140 times suppression of the thermal volatility. In a similar way, the volatilization of **MTL** was suppressed by a factor of >70 upon encapsulation by **1** (Fig. S47†).[11]

Moreover, encapsulated CMTs (*i.e.*, **MTL** and **MTO**) in the cavity of solid **1** hardly volatilized even under high vacuum at elevated temperature (*i.e.*, 480 Pa and 80 °C) for 1 h, as confirmed by $^1$H NMR analysis (Fig. 6d and e). In contrast, free **MTL** and **MTO** volatilized instantly (<4 min) under the same conditions.[23] Thermal gravimetric (TG) analysis of solid **1**·**MTO** showed 4.4% weight loss in the range of 88–200 °C, assignable to the release of the encapsulated **MTO** (Fig. S49†). The present results demonstrated that **1** acts as an excellent molecular

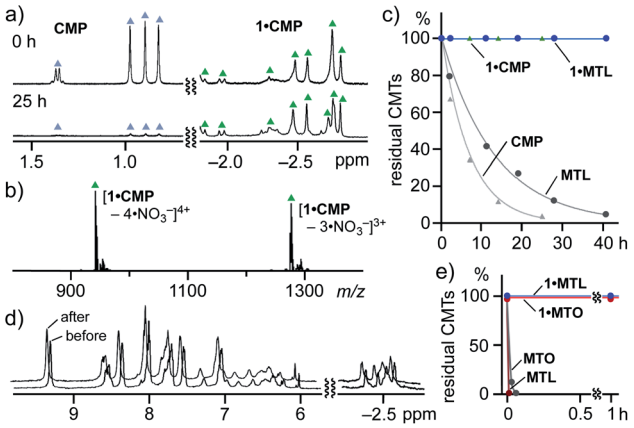


Fig. 6 (a) $^1$H NMR spectra (500 MHz, $D_2O$, r.t.) of free **CMP** and **1**·**CMP** before/after heating at 80 °C for 25 h in water, and (b) ESI-TOF MS spectrum ($H_2O$) of the resultant solution after heating. (c) Time-course profile of the volatilization (%) of **CMP** and **MTL** within/without **1** in water at 80 °C. (d) $^1$H NMR spectra (500 MHz, $D_2O$, r.t.) of **1**·**MTO** before/after heating at 80 °C under vacuum for 1 h in the solid state. (e) Time-course profile of the volatilization (%) of **MTO** and **MTL** within/without **1** in the solid state at 80 °C under vacuum.

storage for volatile CMTs in solution as well as in the solid state.[24]

## Conclusions

We have revealed the new functions of a polyaromatic capsule acting as a nanoflask for cyclic monoterpenes (CMTs) both in solution and in the solid state. Although the recognition of CMTs is highly challenging due to their simple structure and high volatility, the capsule preferentially bound menthone from a mixture of CMTs in water and in the gas phase under ambient conditions. Unusual pair-selective encapsulations of two different CMTs (*e.g.*, menthone and *p*-cymene) were also accomplished by the capsule. Moreover, the capsule prompted the thermal isomerization of menthone and largely suppressed the volatilities of CMTs in the confined cavity. This level of control over CMTs has not been accomplished with previous molecular receptors[5–8] and solid materials.[25] We hope that the present work will open the door to new host–guest chemistry of polyaromatic nanoflasks[26] toward not only natural but also synthetic volatile compounds.

## Author contributions

R. S., Y. T., K. N., S. T., and M. Y. designed the work, carried out research, analyzed data, and wrote the paper. Y. S. contributed to crystallographic analysis. M. Y. is the principal investigator. All authors discussed the results and commented on the manuscript.

## Conflicts of interest

There are no conflicts to declare.

## Acknowledgements

This work was supported by JSPS KAKENHI (Grant No. JP18H01990/JP19H04566) and "Support for Tokyo Tech Advanced Researchers (STAR)". The computations were performed using computers in Research Center for Computational Science, Okazaki, Japan.

## Notes and references

1 C. Sell in *Handbook of Essential Oils Science, Technology, and Applications*, ed K. H. C. Başer and G. Buchbauer, CRC Press, 2009, pp. 131–135.
2 P. K. Ajikumar, K. Tyo, S. Carlsen, O. Mucha, T. H. Phon and G. Stephanopoulos, *Mol. Pharm.*, 2008, 167–190.
3 A. G. Guimarães, J. S. S. Quintans and L. J. Quintans-Júnior, *Phytother Res.*, 2013, **27**, 1–15.
4 Z. Jiang, C. Kempinski and J. Chappell, *Curr. Protoc. Plant Biol.*, 2016, **1**, 345–358.
5 (*a*) C. Donze and A. W. Coleman, *J. Inclusion Phenom. Mol. Recognit. Chem.*, 1996, **16**, 1–15; (*b*) G. Ramon, A. W. Coleman and L. R. Nassimbeni, *Cryst. Growth Des.*, 2006, **6**, 132–136; (*c*) M. A. Romero, N. Basílio, A. J. Moro, M. Domingues, J. A. González-Delgado, J. F. Arteaga and U. Pischel, *Chem.–Eur. J.*, 2017, **23**, 13105–13111.
6 (*a*) Y. Tokunaga and J. Rebek Jr, *J. Am. Chem. Soc.*, 1998, **120**, 66–69; (*b*) J. L. Bolliger, T. K. Ronson, M. Ogawa and J. R. Nitschke, *J. Am. Chem. Soc.*, 2014, **136**, 14545–14553.
7 A. Suzuki, K. Kondo, Y. Sei, M. Akita and M. Yoshizawa, *Chem. Commun.*, 2016, **52**, 3151–3154.
8 Recent reviews on coordination cages and capsules: (*a*) T. R. Cook and P. J. Stang, *Chem. Rev.*, 2015, **115**, 7001–7045; (*b*) C. J. Brown, F. D. Toste, R. G. Bergman and K. N. Raymond, *Chem. Rev.*, 2015, **115**, 3012–3035; (*c*) L.-J. Chen, H.-B. Yang and M. Shionoya, *Chem. Soc. Rev.*, 2017, **46**, 2555–2576; (*d*) I. Sinha and P. S. Mukherjee, *Inorg. Chem.*, 2018, **57**, 4205–4221; (*e*) F. J. Rizzuto, L. K. S. von Krbek and J. R. Nitschke, *Nat. Rev. Chem.*, 2019, **3**, 204–222; (*f*) H. Sepehrpour, W. Fu, Y. Sun and P. J. Stang, *J. Am. Chem. Soc.*, 2019, **141**, 14005–14020; (*g*) A. B. Grommet, M. Feller and R. Klajn, *Nat. Nanotechnol.*, 2020, **15**, 256–271; (*h*) E. G. Percástegui, T. K. Ronson and J. R. Nitschke, *Chem. Rev.*, 2020, **120**, 13480–13544; (*i*) K. Ariga and M. Shionoya, *Bull. Chem. Soc. Jpn.*, 2021, **94**, 839–859.
9 (*a*) N. Kishi, Z. Li, K. Yoza, M. Akita and M. Yoshizawa, *J. Am. Chem. Soc.*, 2011, **133**, 11438–11441; (*b*) M. Yoshizawa and L. Catti, *Acc. Chem. Res.*, 2019, **52**, 2392–2404.
10 (*a*) M. Yamashina, S. Matsuno, Y. Sei, M. Akita and M. Yoshizawa, *Chem.–Eur. J.*, 2016, **22**, 14147–14150; (*b*) M. Yamashina, M. Akita, T. Hasegawa, S. Hayashi and M. Yoshizawa, *Sci. Adv.*, 2017, **3**, e1701126; (*c*) S. Kusaba, M. Yamashina, M. Akita, T. Kikuchi and M. Yoshizawa, *Angew. Chem., Int. Ed.*, 2018, **57**, 3706–3710; (*d*) M. Yamashina, T. Tsutsui, Y. Sei, M. Akita and M. Yoshizawa, *Sci. Adv.*, 2019, **5**, eaav3179; (*e*) K. Niki, T. Tsutsui, M. Yamashina, M. Akita and M. Yoshizawa,

*Angew. Chem., Int. Ed.*, 2020, **59**, 10489–10492; (*f*) H. Dobashi, L. Catti, Y. Tanaka, M. Akita and M. Yoshizawa, *Angew. Chem., Int. Ed.*, 2020, **59**, 11881–11885; (*g*) T. Tsutsui, L. Catti, K. Yoza and M. Yoshizawa, *Chem. Sci.*, 2020, **11**, 8145–8150.

11 See the ESI.† Pale-yellow single crystals were obtained by slow concentration of the $H_2O$ solutions of **1·MTO** and **1·CMP** at room temperature for ~40 d.

12 The ITC analysis of **1·CMP** also revealed its thermodynamic parameters (*i.e.*, $\Delta H = -14.9$ kJ mol$^{-1}$, $T\Delta S = 15.8$ kJ mol$^{-1}$ (25 °C), and $K_a = 2.4 \times 10^5$ M$^{-1}$; Fig. S21 and Table S1†).[11]

13 (*a*) D. P. August, C. S. Nichol and P. J. Lusby, *Angew. Chem., Int. Ed.*, 2016, **128**, 15246–15250; (*b*) V. Martí-Centelles, A. L. Lawrence and P. J. Lusby, *J. Am. Chem. Soc.*, 2018, **140**, 2862–2868; (*c*) T. A. Young, V. Martí-Centelles, J. Wang, F. Duarte and P. J. Lusby, *J. Am. Chem. Soc.*, 2020, **142**, 1300–1310.

14 Pair-selective encapsulation of biomolecules by a synthetic host is very rare: P. Mateus, N. Chandramouli, C. D. Mackereth, B. Kauffmann, Y. Ferrand and I. Huc, *Angew. Chem., Int. Ed.*, 2020, **59**, 5797–5805.

15 Ternary complex **1**·(**MTO**·**CMN**) is not stable enough under the MS condition and thus MS peaks derived from **1·MTO** were observed at $m/z$ = 942.8 and 1278.0 (Fig. 3e and S29†). Theoretical studies of the host–guest complexes indicated that the formation of **1**·(**MTO**·**CMN**) is more favorable (>25 kJ mol$^{-1}$) than that of **1·MTO** or **1**·(**CMN**)$_2$ in the gas phase (Fig. S31†).

16 The $^1$H NMR, $^1$H–$^1$H COSY, and HSQC analyses of **1·MTO** after the thermal treatment indicated the formation of three isomers of MTO, besides the diequatorial chair form (Fig. S35a–c†).

17 The activation energy ($\Delta G^{\ddagger}$) of the thermal isomerization of **MTO** within **1** was estimated to be 92.8 kJ mol$^{-1}$ at 303 K, by the Eyring plots (Fig. S37†).

18 The conformational isomers of **MTO** (20 structures) were initially generated through automatic conformational analysis using Conflex 8, Rev. C program and subsequently their optimized structures and energies were obtained by DFT calculations (CAM-B3LYP/6-31G(d) level of theory, gas phase; Fig. S40a†). Furthermore, the optimized structures and energies were obtained from the host–guest complexes, using **1** (R = –$OCH_3$) and the most stable four conformers of **MTO**, by DFT calculations (CAM-B3LYP/LanL2DZ (for Pt), 6-31G(d) (for C, H, N, O) level of theory, gas phase for optimization and PCM($H_2O$) for estimation of energies; Fig. S40b†).

19 Stabilization of the axial conformer of chlorocyclohexane in the crystalline state: S. Hirano, S. Toyota, M. Kato and F. Toda, *Chem. Commun.*, 2005, 3646–3648.

20 (*a*) M. Squillacote, R. S. Sheridan, O. L. Chapman and F. A. L. Anet, *J. Am. Chem. Soc.*, 1975, **97**, 3244–3246; (*b*) G. Gill, D. M. Pawar and E. A. Noe, *J. Org. Chem.*, 2005, **70**, 10726–10731; (*c*) A. Krin, C. Pérez, P. Pinacho, M. M. Quesada-Moreno, J. J. López-González, J. R. Avilés-Moreno, S. Blanco, J. C. López and M. Schnell, *Chem.–Eur. J.*, 2018, **24**, 721–729.

21 Gas molecules bound by coordination cages in solution: (*a*) I. A. Riddell, M. M. J. Smulders, J. K. Clegg and J. R. Nitschke, *Chem. Commun.*, 2011, **47**, 457–459; (*b*) J. Roukala, J. Zhu, C. Giri, K. Rissanen, P. Lantto and V.-V. Telkki, *J. Am. Chem. Soc.*, 2015, **137**, 2464–2467; (*c*) C. Browne, W. J. Ramsay, T. K. Ronson, J. Medley-Hallam and J. R. Nitschke, *Angew. Chem., Int. Ed.*, 2015, **54**, 11122–11127; (*d*) L. Ma, C. J. E. Haynes, A. B. Grommet, A. Walczak, C. C. Parkins, C. M. Doherty, L. Longley, A. Tron, A. R. Stefankiewicz, T. D. Bennett and J. R. Nitschke, *Nat. Chem.*, 2020, **12**, 270–275.

22 (*a*) D. Preston, K. F. White, J. E. M. Lewis, R. A. S. Vasdev, B. F. Abrahams and J. D. Crowley, *Chem.–Eur. J.*, 2017, **23**, 10559–10567; (*b*) J. S. Wright, A. J. Metherell, W. M. Cullen, J. R. Piper, R. Dawson and M. D. Ward, *Chem. Commun.*, 2017, **53**, 4398–4401.

23 Free **MTO** volatilized over 25 min at atmospheric temperature and pressure (Fig. S48e†).

24 (*a*) β-Cyclodextrin and its derivative show weak volatile suppression effects in water (e.g., ~50% loss of **CMP** at 60 °C for 100 min and 60% loss of **MTL** at 40 °C for 5 h); (*b*) M. Tanaka, H. Matsuda, H. Sumiyoshi, H. Arima, F. Hirayama, K. Uesaka and S. Tsuchiya, *Chem. Pharm. Bull.*, 1996, **44**, 416–420; (*c*) N. Ajisaka, K. Hara, K. Mikuni, K. Hara and H. Hashimoto, *Biosci., Biotechnol., Biochem.*, 2000, **64**, 731–734.

25 (*a*) T. Gruber, C. Fischer, W. Seichter, P. Bombicz and E. Weber, *CrystEngComm*, 2011, **11**, 1422–1431; (*b*) J. Zhang, M. Yu, P. Yuan, G. Lu and C. Yu, *J. Inclusion Phenom. Macrocyclic Chem.*, 2011, **71**, 593–602.

26 Reviews on polyaromatic capsules, cages, and tubes: (*a*) M. Yoshizawa and M. Yamashina, *Chem. Lett.*, 2017, **46**, 163–171; (*b*) K. Yazaki, L. Catti and M. Yoshizawa, *Chem. Commun.*, 2018, **54**, 3195–3206.